

In vivo optical imaging with $Y_2O_3S:Eu:Mg:Ti$ persistent luminescent nanoparticles

XU CAO, YUZHONG GONG SHOUPIPING ZHU, XUANXUAN ZHANG XUELI CHEN, YONGHUA ZHAN*

Engineering Research Center of Molecular and Neuro Imaging of the Ministry of Education & School of Life Science and Technology, Xidian University, Xi'an, Shaanxi 710071, China

Fluorescence imaging is widely used for *in vivo* imaging and has provided remarkable results. However, tissue auto-fluorescence and external illumination limit the SNR and resolution. Persistent luminescent nanoparticles can emit afterglow for several minutes to hours after they are excited. Therefore persistent luminescent imaging based on these materials can circumvent tissue auto-fluorescence and external illumination during detection and obtain images with high SNR and resolution. $Y_2O_3S:Eu:Mg:Ti$ is a red persistent luminescent material, which has a highly efficient luminescence and stable chemical property. This work investigates the feasibility of $Y_2O_3S:Eu:Mg:Ti$ nanoparticles in small animal imaging of lymph node and bio-distribution.

(Received September 4, 2017; accepted August 9, 2018)

Keywords: Persistent luminescent imaging, $Y_2O_3S:Eu:Mg:Ti$ nanoparticles, Fluorescence imaging

1. Introduction

With the emergence of a variety of optical probes, optical molecular imaging can provide non-invasive and real-time observations of small animals. A recently developed optical probe, persistent luminescent nanoparticles (PLNP) can emit light for several minutes to hours after excitation [1]. For *in vivo* imaging, persistent luminescent imaging based on PLNP can significantly improve SNR and resolution due to non-disturbance from excitation light and auto-fluorescence [2]. PLNP has been widely used in imaging of tumor bearing mouse [3-7].

Light in tissue transparency window (wavelength from 700 nm to 1000 nm) has a weak attenuation in biological tissues due to scattering much stronger than absorption [8]. So many researchers focus on red PLNP [9-13]. $Y_2O_3S:Eu:Mg:Ti$ (YOS) is a kind of red persistent luminescent phosphors which has a highly efficient luminescence, stable chemical property [14-16]. Ti and Mg were doped into $Y_2O_3S:Eu$, and a new persistent luminescent phosphor YOS had a better luminescent property and attracted more attentions [17-19].

Although the YOS phosphor is currently one of the best red afterglow materials, there is little report about *in vivo* imaging using this material. Therefore this work focuses on investigating the feasibility of YOS nanoparticles in small animal imaging of lymph node and bio-distribution.

2. Experimental

2.1. Characterization of YOS nanoparticles

YOS nanoparticles with average size of 100 nm were purchased from Yao dexing technology co. Ltd (Shenzhen, China). Normal nude mice were purchased from Vital River Laboratory Animal Technology Co., Ltd. (Beijing, China).

The XRD pattern of YOS nanoparticles was measured with an X-ray diffractometer (DX-1000, Dandong Fangyuan Instrument Co. Ltd., Dandong, China). The emission spectra of YOS nanoparticles were determined using a Hitachi F-7000 fluorometer (Hitachi, Japan) after excited by a UV lamp (3 W lamp, 265 nm) for 90S.

Five small plates with the same concentration (100 $\mu\text{g/mL}$ in PBS at pH 7.4) and volume of (0.2 mL) of YOS nanoparticles were prepared to investigate the excitation characterization of YOS nanoparticles. To avoid the interference of background persistent luminescence of YOS nanoparticles excited by ambient sunlight, all the samples were stayed in dark environment for 2 hours. For each excitation case we took out one sample and excited it with a UV lamp for a specific duration. Then we closed the UV lamp and immediately captured the persistent luminescence image using an EMCCD camera (iXon Ultra 888, Andor Technology Ltd., Belfast, UK) coupled with a focus lens (Xenon 25 mm f/0.95, Schneider Optics, Inc., CA, USA) with EM gain of 50 and exposure time of 1s in a homemade light tight imaging chamber.

To investigate the emission property of YOS

nanoparticles. A small plate with 0.2 mL YOS nanoparticles with the concentration of 100 $\mu\text{g}/\text{mL}$ was irradiated by 265 nm UV lamp for 120s. Then serial persistent luminescence images were acquired immediately in sequence mode with the frequency of 0.5 Hz. The acquisition parameters of EM gain and exposure time were set to 50 and 1s, respectively.

2.2. In vivo imaging

Animal experiments were performed in accordance with the guidelines of the National Regulation of China for Care and Use of Laboratory Animals. All procedures for *in vivo* imaging were approved by the Xidian University Animal Care and Use Committee.

Two normal BALB/C mice were anesthetized with intraperitoneal administration of 4% chloral hydrate at a dosage of 400 $\text{mg} \cdot \text{kg}^{-1}$. YOS with the concentration of 100 $\mu\text{g}/\text{mL}$ in PBS at pH 7.4 was pre-irradiated by 265 nm UV lamp for 90s.

For *in vivo* lymph node imaging, 0.1 mL the pre-irradiated YOS was subcutaneous injected into the right footpad of an anesthetized normal BALB/C mouse. Serial persistent luminescence images were acquired

immediately for the first 5 minutes with the frequency of 0.5 Hz. 1 hour after pre-irradiation, we irradiated the mouse using 265 nm UV lamp again and acquired a single persistent luminescence image. The acquisition parameters of EM gain and exposure time were set to 100 and 0.5s, respectively.

For *in vivo* bio-distribution imaging, 0.2 mL pre-irradiated YOS was subcutaneous injected through tail vein of an anesthetized normal BALB/C mouse. Serial persistent luminescence images were acquired immediately for 5 minutes with the frequency of 0.5 Hz using the same setups for the EMCCD camera. About 1 hour post-intravenous injection of YOS, *Ex vivo* persistent luminescence images of isolated organs were also captured.

3. Results and discussion

The XRD pattern is shown in Fig. 1 (a). Compared with $\text{Y}_2\text{O}_2\text{S}$ in JCPDS standard card, the XRD image of YOS is in accordance with the standard spectra. The Fig. 1 (b) shows the persistent luminescence spectrum of YOS when excited by 265 nm UV light. YOS exhibits an emission peaking at 630 nm.

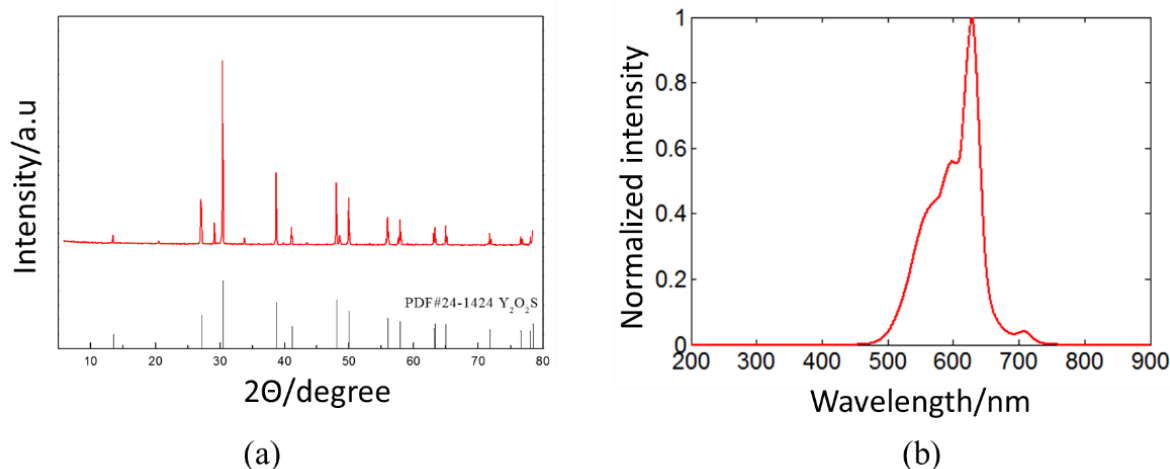


Fig. 1. Characterization of YOS nanoparticles. (a) XRD patterns; (b) persistent luminescence spectrum excited by 265 nm UV light

The initial persistent luminescence images for different excitation durations are shown at the top of Fig. 2(a). 20% of the maximum was used as the threshold and the region of interesting (ROI) was defined by the pixels which were less than the threshold. The average counts of ROI varied with excitation durations is also provided at the bottom of Fig. 2(a), which is defined as the excitation

curve. This excitation curve fits an exponent function $y=3147e^{-3/t}+1813$. The initial intensity of persistent luminescence image almost gets to saturation when the excitation duration longer than 90s. So the optimized excitation duration for YOS is 90s to reach a relatively bright persistent luminescence image.

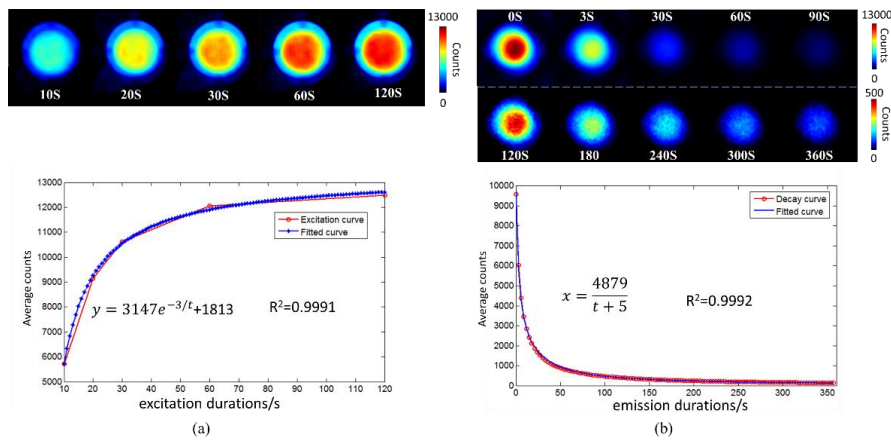


Fig. 2. Excitation and emission characterization of YOS nanoparticles. (a) The initial persistent luminescence images for different excitation durations (top), the excitation curve (bottom); (b) The persistent luminescence images for different time points (top), the emission curve (bottom)

The persistent luminescence images at different time points are shown at the top of Fig. 2(b). The average counts of ROI varied with emission durations is also provided at the bottom of Fig. 2(b), and the decay curve fits an function $y = 4879 / (t + 5)$. In the first 60S, the decay curve decreases very fast. The lasting time of YOS is about 5 minutes. This lasting time is long enough for acquiring a persistent luminescence image after close of excitation light.

In the Fig. 3 (a), the popliteal lymph node can clearly be seen in persistent luminescence image 1 minute after injection of YOS. 1 hour later, the mouse was excited by the 265 nm UV lamp again, and we also captured gastric lymph node as shown in Fig. 3 (b). The signal of gastric lymph node is much stronger than that of popliteal lymph node. That means most the YOS nanoparticles have circulated to gastric lymph node.

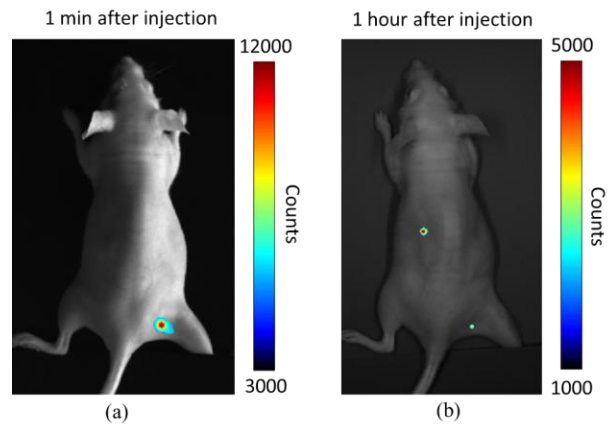


Fig. 3. Lymph node imaging. (a) Popliteal lymph node; (b) Gastric lymph node and popliteal lymph node

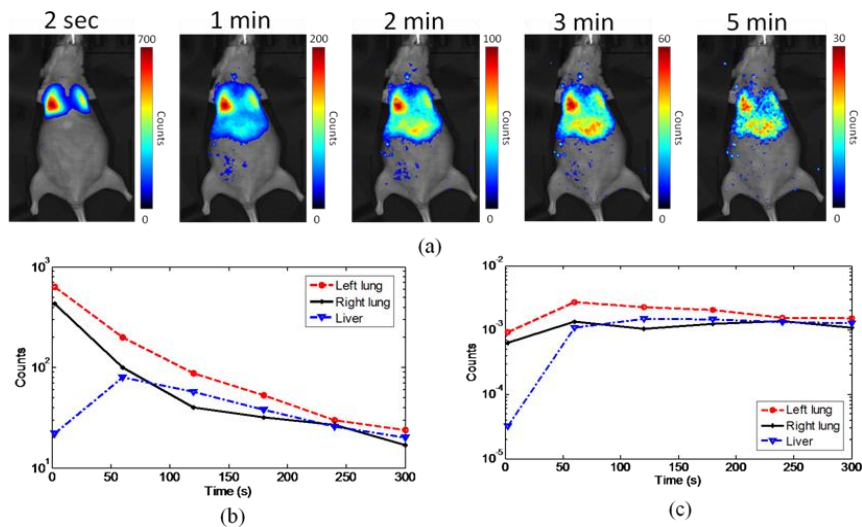


Fig. 4. Persistent luminescence imaging of bio-distribution. (a) Persistent luminescence images at different time points; (b) Quantified curve without calibration by the decrease curve of YOS; (c) Quantified curve after calibration by the decrease curve of YOS

Fig. 4(a) shows the persistent luminescence images captured at different time points. After injection through tail vein, YOS reached the lungs immediately. And then, YOS gradually gets into liver with blood circulation. Quantified curves of lungs and liver also were also provided in Fig. 4(b) and Fig. 4(c). Because the decreasing properties of PL signals with time, so before calibration

with the decrease curve of YOS it is difficult to give the concentration information of YOS. Fig. 4(c) can really demonstrates the concentrations of YOS in different organs. YOS increases in lungs and liver in the first 60 seconds, and they decrease gradually with time after 60 second time point.

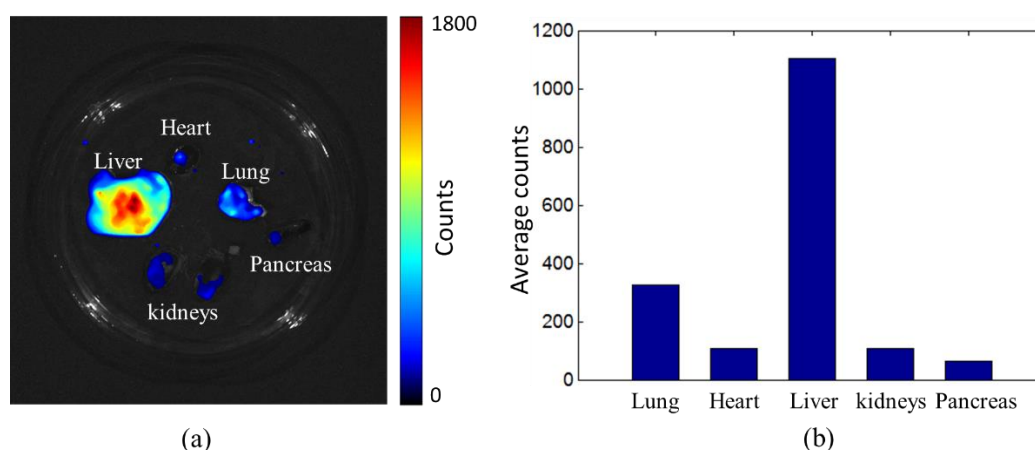


Fig. 5. Ex vivo persistent luminescence images of isolated organs from a normal mouse at 5 hour post-intravenous injection of YOS nanoparticles

After 5 hours of circulation, the mouse was dissected and the organs were removed. All the isolated organs were excited by the 265 nm UV lamp. Then we obtained the *ex-vivo* persistent luminescence images of isolated organs as shown in Fig. 5 (a). YOS mainly distributes in liver and lungs. Quantified analysis is also provided in Fig. 5 (b).

4. Conclusions

In conclusion, we have reported the YOS nanoparticles for *in vivo* persistent luminescence imaging. For small animal *in vivo* imaging, without interruption of excitation light and auto-fluorescence, persistent luminescence imaging could be served as a new potential platform to obtain a high SNR, low noise, and good spatial resolution image. This work focuses on lymph node and bio-distribution studies, because YOS nanoparticles have no tumor targeted properties. So our future work will aim to synthesize functional YOS nanoparticles and extend its *in vivo* applications.

Acknowledgements

This work was supported by the Program of National Natural Science Foundation of China under Grant Nos. 81227901, 81627807, 61405149, 81230033, and 61471279, the Program of the National key Research and

Development Program of China under Grant No. 2016YFC0103802.

References

- [1] T. Aitasalo, P. Deren, J. Hölsä, H. Jungner, J. C. Krupa, M. Lastusaari, J. Legendziewicz, J. Niittykoski, W. Strek, J. Solid State Chem. **171**, 114 (2003).
- [2] Z. Pan, Y. Y. Lu, F. Liu, Nat. Mater. **11**, 58 (2011).
- [3] Q. le Masne de Chermont, C. Chanéac, J. Seguin, F. Pellé, S. Maîtrejean, J. P. Jolivet, D. Gourier, M. Bessodes, D. Scherman, Proc. Natl. Acad. Sci. U.S.A. **104**, 9266 (2007).
- [4] T. Maldiney, C. Richard, J. Seguin, N. Wattier, M. Bessodes, D. Scherman, ACS Nano **5**, 85 (2011).
- [5] T. Maldiney, M. U. Kaikkonen, J. Seguin, Q. le Masne de Chermont, M. Bessodes, K. J. Airene, S. Ylä-Herttuala, D. Scherman, C. Richard, Bioconjug. Chem. **23**, 472 (2012).
- [6] A. Abdukayum, J. T. Chen, Q. Zhao, X. P. Yan, J. Am. Chem. Soc. **135**, 14125 (2013).
- [7] T. Maldiney, A. Bessière, J. Seguin, E. Teston, S. K. Sharma, B. Vana, A. J. Bos, P. Dorenbos, M. Bessodes, D. Gourier, D. Scherman, C. Richard, Nat. Mater. **13**, 418 (2014).
- [8] W. F. Cheong, S. A. Prahl, A. J. Welch, IEEE J. Sel. Top. Quant. **26**, 2166 (1990).

- [9] T. Matsuzawa, Y. Aoki, N. Takeuchi, Y. Murayama, *Journal of the Electrochemical Society* **143**, 2670 (1996).
- [10] M. Kamada, J. Murakami, N. Ohno, *Journal of Luminescence* **25**, 1042 (2000).
- [11] Y. H. Lin, Z. T. Zhang, F. Zhang, Z. L. Tang, *Materials Chemistry and Physics* **65**, 103 (2000).
- [12] L. M. Liu, L. H. Zeng, S. X. Lian, J. H. Zhang, X. H. Mao, *Hunan Nonferrous Metals* **14**, 45 (1998).
- [13] F. Jie, *Electrochemical and Solid-State Letters* **3**, 350 (2000).
- [14] L. E. Sobon, K. A. Wickersheim, R. A. Buchanan, *Journal of Applied Physics* **42**, 3049(1971).
- [15] C. H. Kang, R. S. Liu, J. C. Chang, *Cheminform* **35**, 3966 (2003).
- [16] J. Dhanaraj, M. Geethalakshmi, R. Jagannathan, *Chemical Physics Letters* **387**, 23 (2004).
- [17] W. Li, Y. Liu, P. Ai, X. Chen, *Journal of Rare Earths* **27**, 895 (2009).
- [18] C. E. Cui, H. Liu, P. Huang, *Optical Materials* **36**, 495 (2013).
- [19] C. Cui, G. Jiang, P. Huang, *Ceramics International* **40**, 4725 (2014).

*Corresponding author: yhzhan@xidian.edu.cn